La mer 42 : 73–82, 2004
Société franco-japonaise d'océanographie, Tokyo

A numerical experiment on the coastal and bottom topographic effects of the Tokara Strait on the Kuroshio flow

Miao Yang CHEN* and Yoshihiko SEKINE*

Abstract : Coastal and bottom topographic effects of the Tokara Strait south of Kyushu on the Kuroshio flow are studied by use of a two layer numerical model. It is shown that a western region of the Tokara Strait is essentially considered as a separation region of the Kuroshio from the western boundary in the East China Sea and an anticyclonic eddy is formed in the separation region. It is also shown that the southwestward flow along the continental slope off Nansei Islands is formed in the lower layer by the topographic guiding effect along the isopleth of depth. The southwestward flow is also formed in a flat bottom model during the spin-down period of the cyclonic eddy. This southwestward flow is an opposite direction to the northeastward Ryukyu Current, which is not modeled in this study. As the Ryukyu Current is essentially formed as a barotropic response to the seasonal change in wind stress, the vertically homogeneous flow is expected. It is suggested that the Ryuku Current is blocked by this southwestward flow and the vertical velocity change (vertical velocity shear) is generated in the Ryukyu Current, which agrees with the observational evidence.

Keywords *: Tokara Strait, Ryukyu Current, Topographic effect*

1. Introduction

It has been widely accepted that the Kuroshio has a bimodal path characteristics in the Shikoku Basin between a non-large meander path and a large meander path (e.g. TAFT, 1972; NITANI, 1975; ISHII *et al.*, 1983). Recently, the difference in the horizontal velocity distribution of the Kuroshio through the Tokara Stait south of Kyushu was especially noticed as an important parameter of the selection of the bimodal path of the Kuroshio. AKITOMO *et al.* (1991, 1997) numerically showed that the northward shift of the main Kuroshio axis in southwest to Kyushu is formed during the large meander path. A similar tendency is also shown by observational data analyses (e.g., KAWABE, 1995; YAMASHIRO and KAWABE, 1996, 2002; OKA and KAWABE, 2003). As the simplified flat bottom is assumed in the numerical models of AKITOMO *et al.* (1991, 1997), more detailed discussion on the coastal and bottom topographic effects of the Tokara Strait is needed to draw firm conclusion on this problem.

In the present study, a realistic topography of the Tokara Strait and Shikoku Basin south of Japan are modeled and the coastal and bottom topographic effects of the Tokara Strait on the velocity distribution of the Kuroshio is examined. ZHANG and SEKINE (1995ab) modeled realistic coastal and bottom topographies south of Japan and examined the path dynamics of the Kuroshio. However, since the inflow of the numerical model was given at the western region of the Tokara Strait, detailed coastal and bottom topographic effects of the Tokara Strait have not been examined. Therefore, the inflow of the numerical model is given at east of Taiwan in the present study and the topographic effects of Tokara Strait is examined.

Some numerical models with different model characteristics are performed in the present

* Institute of Physical Oceanography, Faculty of Bioresources, Mie University, Tsu 514–8507, Japan

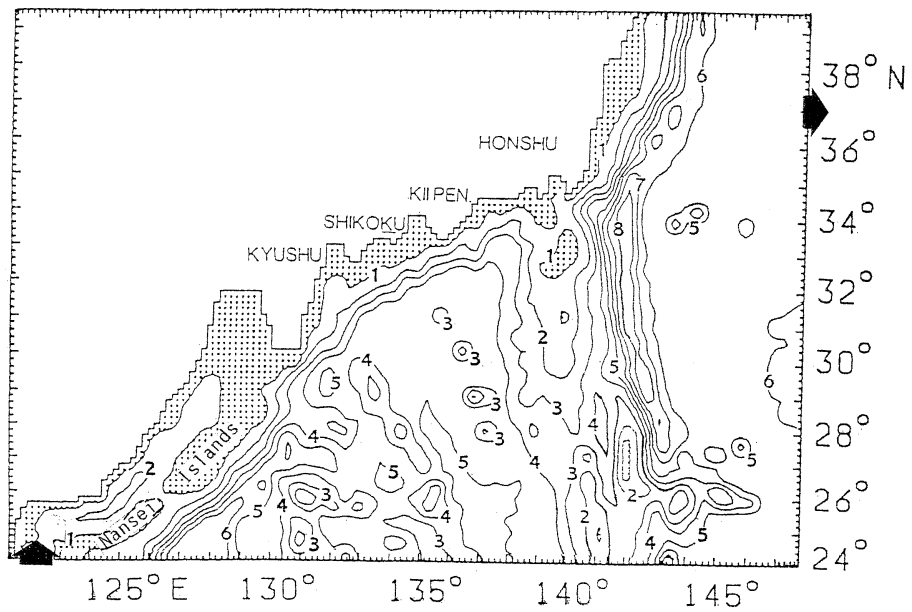

Fig. 1. Schematic view of the model ocean shown by the isopleth of depth (in 1000 m). Two arrows show the region of the in-and outflow and regions shallower than 1000 m are stippled.

study and the coastal topographic and bottom topographic effects are examined independently. Namely, the coastal topographic effect is examined by the flat bottom model and the bottom topographic effect is examined by the realistic bottom model, depending on the intensity of the current velocity of in- and outflow. In the followings, the details of the numerical model and characteristics of each model are described in the next section. The results of the numerical experiments are mentioned in sections 3, summary and discussion are made in section 4.

2. Numerical model

A two layer ocean with bottom and coastal topographies shown in Fig. 1 is employed in this study. Here, an isopleth of the depth of 150 m is assumed as the coastal boundary in the East China Sea. The reduced gravity of the two layer model is assumed to be 2.87×10^{-2}msec^{-2}. The basic equations are the same as those of ZHANG and SEKINE (1995ab). The system is driven by stationary in- and outflow through the open boundary.

As for the initial state, the flow is given only in the upper layer and the lower layer has no motion (Fig.2). Sinusoidal horizontal velocity distribution of in- and outflow is assumed and only northward (eastward) velocity component is given at the inflow (outflow) boundary. A viscous boundary condition is imposed on the northern coastal boundary and a slip boundary condition is imposed on the other open boundaries. In the numerical calculation, we adopt a rectangular grid with horizontal spacing of 18.7 Km along x - axis (eastward) and 15.8 Km along y - axis (northward).

In the present study, 8 cases of numerical experiments with different model character are performed. Firstly, a flat bottom with the coastal topography of Fig. 1 and with a constant depth of 3800 m is assumed and the coastal topographic effect is mainly examined. Here, the different in- and outflow volume transport of 30 Sv (1 Sv = 10^6m^3 sec^{-1}), 55 Sv, 70 Sv and 80 Sv is given and the effect of nonlinear effect (advection) is also examined. The four models with different in- and outflow are referred to as F30, F55, F70 and F80. The range of in- and outflow volume transport of the Kuroshio, 30 Sv to 80 Sv, is essentially based on

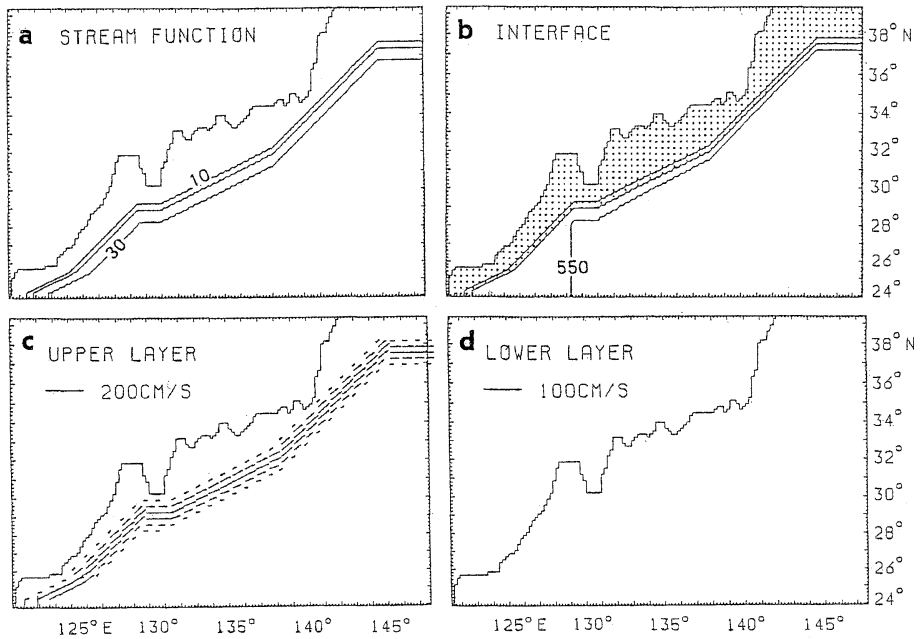

Fig. 2. Initial condition of F30. Spatial distribution of (a) volume transport function, (b) upper layer thickness, (c) velocity fields of upper layer and (d) those of lower layer. The contour intervals of the volume transport function and the upper layer thickness are 10 Sv and 50 m, respectively. Areas with negative volume transport function or thinner upper layer less than 500 m are stippled.

the observed geostrophic flow observations of 35 Sv–55 Sv (Isobe and IMAWAKI, 2002) and 30 Sv–65 Sv (IMAWAKI *et al.*, 2001) and 40 Sv–90 Sv estimated from the sea level height TOPEX/POSEIDON (IMAWAKI *et al.*, 2001).

Secondly, the realistic coastal and bottom topographies of Fig. 1 are employed and the bottom topographic effect of the continental slope is furthermore examined. Here, similar four models with different in- and outflow volume transport of 30 Sv, 55 Sv, 70 Sv and 80 Sv are carried out and they are referred to as T30, T55, T70 and T80, respectively. As for these four realistic bottom models, coefficient of horizontal eddy viscosity is assumed to be $5\times 10^2 m^2 sec^{-1}$, while a larger value of $1\times 10^3 m^2\ sec^{-1}$ is assumed for the four flat bottom models.

Because the current over a flat bottom is essentially unstable and the enhanced velocity is induced. SEKINE (1992) pointed out by use of a simplified two layer model proposed by IKEDA (1983) that a western boundary current over the flat bottom is baroclinically unstable, while a flow over the continental slope south of Japan is almost stable by the stabilizing effect of the continental slope. Therefore, in order to suppress the enhanced velocity in a flat bottom model, larger coefficient of the eddy viscosity is given for the flat bottom models. The numerical time integration of ten years is carried out for each model and the numerical solutions in the stationary state or quasi-stationary state are analyzed.

3. Results

Results showing the statinary velocity fields of F30 are displayed in Fig. 3. A coastal flow along western and northern coasts is formed in the upper layer and the total flow pattern shows a non-large meander path. In the lower layer, three anticyclonic eddies exist at southeast of Kyushu and south of Shikoku and southeast of Kii Peninsula. The volume transport function showing the total transport in the upper and lower layer and thickness of the upper layer of F30 are shown in Fig. 4. Since the lower layer has a larger layer thickness, velocity fields of the lower layer is relatively

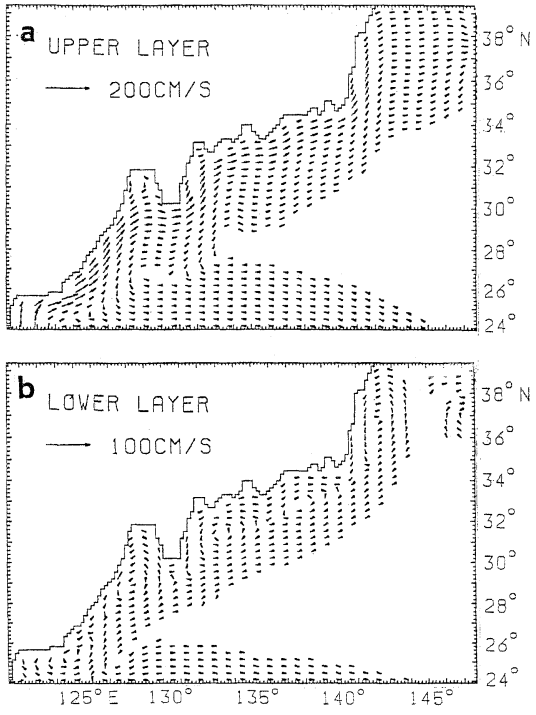

Fig. 3. Result of F30 shown by (a) upper layer velocity and (b) lower layer velocity in a stationary state. No velocity vectors less than 10 cm sec^{-1} in the upper layer and 5 cm sec^{-1} in the lower layer are plotted.

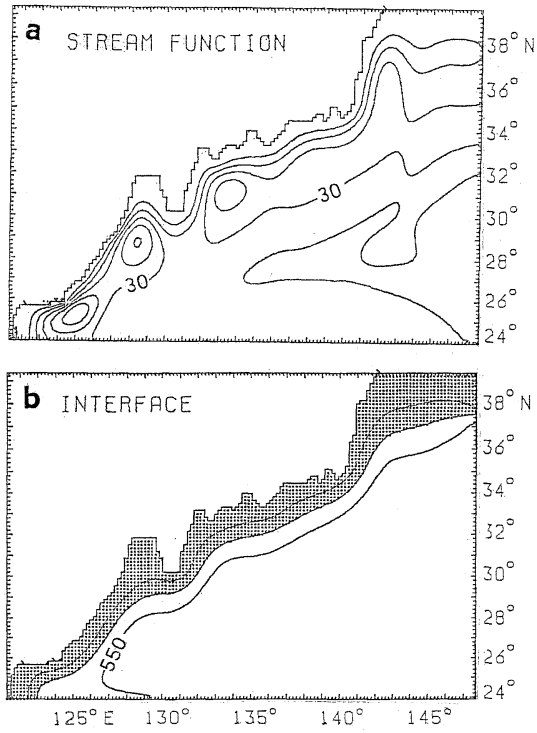

Fig. 4. (a) Volume transport function and (b) the upper layer thickness of F30 in a stationary state. The contour interval is the same as in Fig. 2.

exaggeratedly appeared in the volume transport function. A clear compensation of the surface pressure gradient is not carried out by the gradient of interface in the stationary state (Fig. 4b) and a lower layer velocity is formed (Fig. 3), which indicates the occurrence of the baroclinic instability.

Stationary velocity fields of F55 are shown in Fig. 5. Although essentially similar flow pattern to F30 (Fig. 3) is obtained, amplitude of the meander of the mean flow in the upper layer is enhanced in F55. Two anticyclonic eddies southwest of Kyushu and south of Shikoku are also enhanced in the lower layer and their existence is also detected in the upper layer. A small cyclonic eddy is formed at southeast of Kii Peninsula in the lower layer, which is shown by C in Fig. 5.

In contrast to F30 and F55, a stationary solution is not obtained in F70 and F80. In both cases, a large meander path is essentially formed and a spin-up and spin-down of a cyclonic eddy southeast of Kyushu is repeated (Fig. 6). The large cyclonic eddy is formed in the spin-up periods, while it decays in the spin-down periods. The period of the spin-up and spin-down of the cyclonic eddy is about 50 days for both cases. The flow pattern during the spin-up period of the cyclonic eddy essentially corresponds to the small meander of the Kuroshio southeast of Kyushu (SOLOMON, 1978; SEKINE and TOBA, 1981ab), which is a trigger meander prior to the formation of the large meander path. However, the spin-up and spin-down of the cyclonic eddy in the numerical model give no large influence on the total flow pattern of the Kuroshio south of Kii Peninsula and the large meander path is formed stationary. As for the velocity fields of these models (Fig. 7), a typical large meander path is formed in the upper layer velocity south of Kii Peninsula and the cyclonic eddy accompanied

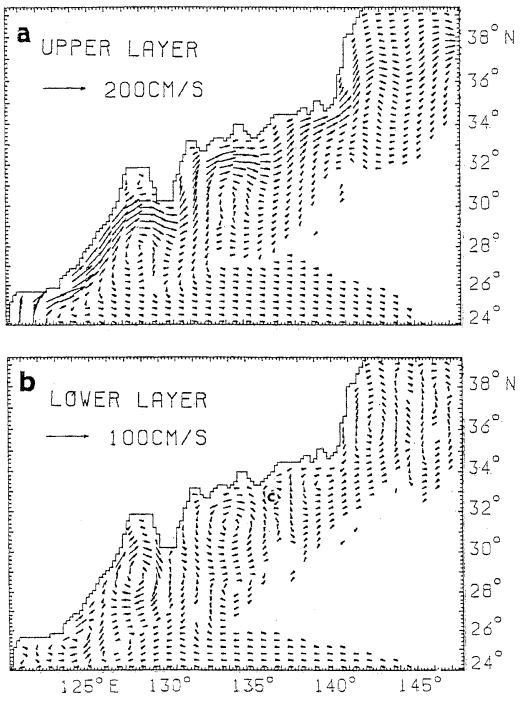

Fig. 5. Same as in Fig. 3 but for F55. The location of the cyclonic eddy southeast of Kii Peninsula in the lower layer is shown by c.

by the large meander path is formed in the lower layer. Two anticyclonic eddies southeast of Kyushu and south of Shikoku are significantly enhanced and they are also clear in the upper layer flow.

It is noted from Figs. 6b,d and 7a that in periods of the spin-down of the cyclonic eddy sothwest of Kyushu, a southwestward flow with a velocity of 30 cm sec^{-1} is formed in the lower layer at the southwestern part of the anticyclonic eddy at the separation area. Although the Ryukyu Current with an approximate maximum velocity of 50 cm sec^{-1} (YUAN *et al.*, 1998) is not modeled in this numerical model, the simulated southwestward flow is the opposite direction to the observed northeastward Ryukyu Current along the continental slope off Nansei Islands. Therefore, it is inferred that the southwestward flow formed in F70 and F80 and the Ryukyu Current blocks each other and their velocities are decreased. In period of the spin-up of the anticyclonic eddy (Figs. 6a,c and 7b), since the anticyclonic eddy develops so eastward and the surrounding flow of the anticyclonic eddy dominates, while the southwestward flow is unclear.

It is also noticed that in F70 and F80 the northward shift of the current path west of Kyushu is more prominent in the upper layer in comparison with those of F30 and F55. Considering that the large meander path is formed in F70 and F80 and the non-large meander path appears in F30 and F55, the northward shift of the current path in case of the large meander path agrees with the observational evidence (KAWABE, 1995; YAMASHIRO and KAWABE, 1996, 2002; OKA and KAWABE, 2003) and the results of the numerical models so far proposed (AKITOMO *et al.*, 1991 and 1997). From the difference of the results between F30–F55 and F70 F80, it is resulted that the formation of the large meander path in F70 and F80 is caused by the northward shift of the current path west of Kyushu and the downstream southward shift by the topographic effect of Kyushu. Namely, because the large northward shift in west of Kyushu yields a large Rossby Lee wave in east to Kyushu, the large meander path has a possibility to be formed as a Rossby Lee wave which induced by the topographic effect of Kyushu.

Although the non-large meander path is formed in F80 of ZHANG and SEKINE (1995a), the large meander path is formed in F80 of this study. Because the non-large meander path in their model is formed by the downstream advection of the large meander, which yields the decay of the large meander path. In the present study, as the inflow is given at east of Taiwan (Fig. 1), the eastward velocity south of Kyushu and its downstream advection of the large meander path are weak and the large meander path is formed. The difference between the two models shows that the range of the non-large meander path in the exceedingly large current velocity of the Kuroshio south of Japan.

Results of T30, T55, T70 and T80 are shown in Fig. 8. Although time dependent quasi-stationary solution is obtained in F70 and F80 (Figs. 6 and 7), the stationary solution is obtained in T70 and T80. All the eddies formed in the flat bottom models are relatively weak and a coastal flow along the western and northern

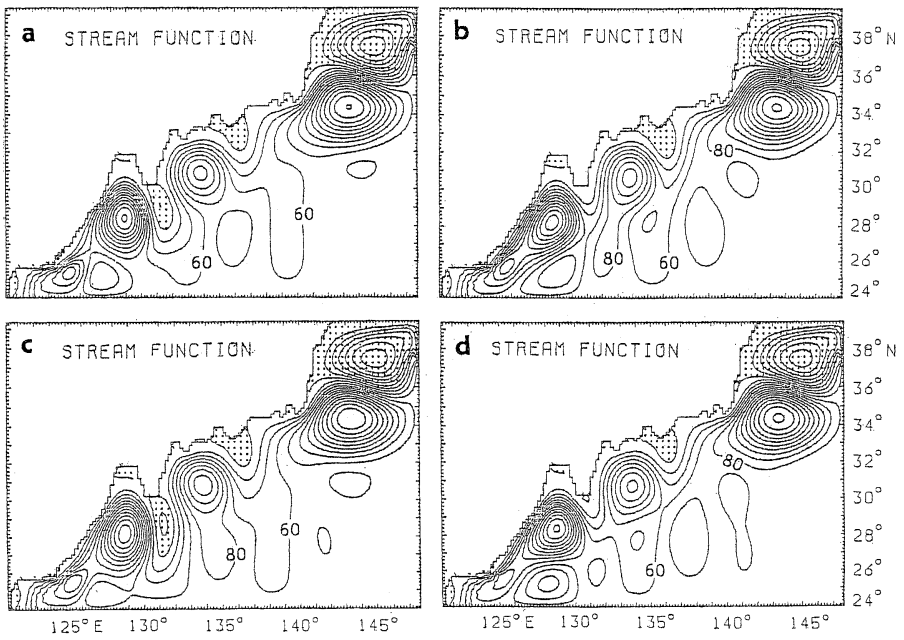

Fig. 6. Time change in the volume transport function of F70 at (a) 1200 days, (b) 1225 days, (c) 1250 days and (d). 1275 days The contour interval of the stream function is 20 Sv. The regions with negative stream function are stippled.

boundaries is formed. In general, the bottom topographic effect is enhanced in a two layer model and the large meander appears in case of significantly large offshore advection effect from continental slope (e.g., SEKINE, 1990). It should be noticed from the lower layer velocity shown in Fig. 9 that the southwestward flow is commonly formed along the continental slope off Nansei Islands. The southwestward flow is maintained stationary and it is confined to the lower layer. Because the lower layer flow has a strong tendency to flow along the contour of f/h, where f is the Coriolis parameter and h is the thickness of the lower layer, which is well approximated by total depth, the southwestward flow along the continental slope off Nansei Islands is generated by the bottom guiding effect along isopleth of depth.

As the northeastward Ryukyu Current flows along the continental slope of the Nansei Islands, the northeastward Ryukyu Current is weakened by the opposite southwestward flow simulated in the present model. Furthermore, the Ryukyu Current is considered as a barotropic response of the ocean to the seasonal change in the wind stress (SEKINE and KUTSUWADA, 1994; KAGIMOTO and YAMAGATA, 1997), the vertically homogeneous flow is expected for the Ryukyu Current. However, it is commonly observed that there exists a vertical velocity change in the Ryukyu Current and the Ryukyu Current is confined to the shallowest margin of the continental slope off Nansei Islands (YUAN *et al.*, 1994, 1998; ZHU *et al*,2003).

As for these observational evidences, it is inferred that the northeastward Ryukyu Current is blocked by the southwestward flow with a vertical velocity shear. Namely, the collision of the southwestward flow and the Ryukyu Current yields the vertical velocity change in the Ryukyu Current. Together with the southwestward flow formed in the flat bottom models, more detailed discussion will be made in the next section.

4. Summary and discussion

We have examined the coastal and bottom topographic effect of Tokara Strait on the

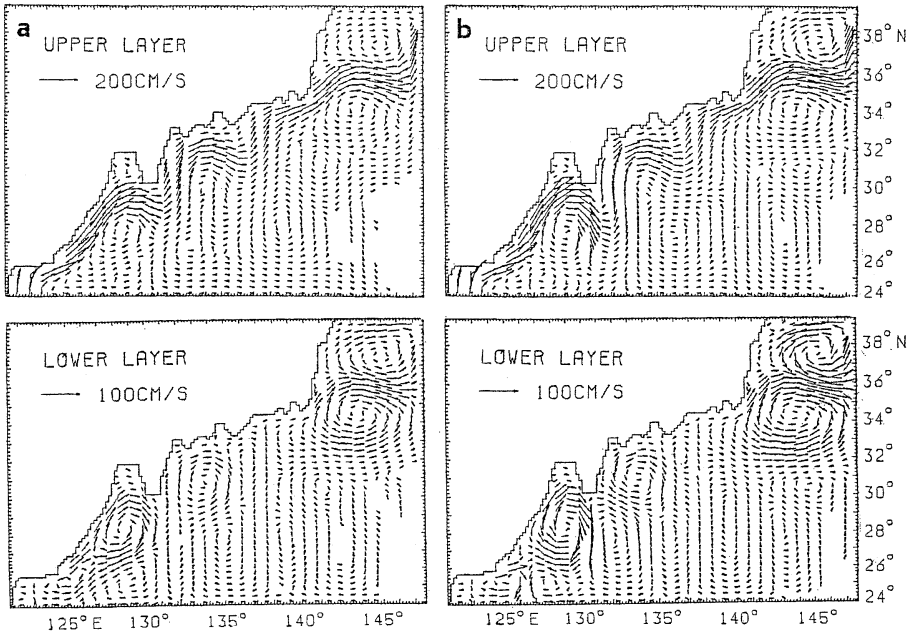

Fig. 7. Velocity fields of F70 (a) in the period of the spin-down of the cyclonic eddy southeast of Kyushu and those (b) in the period of spin-up of the cyclonic eddy.

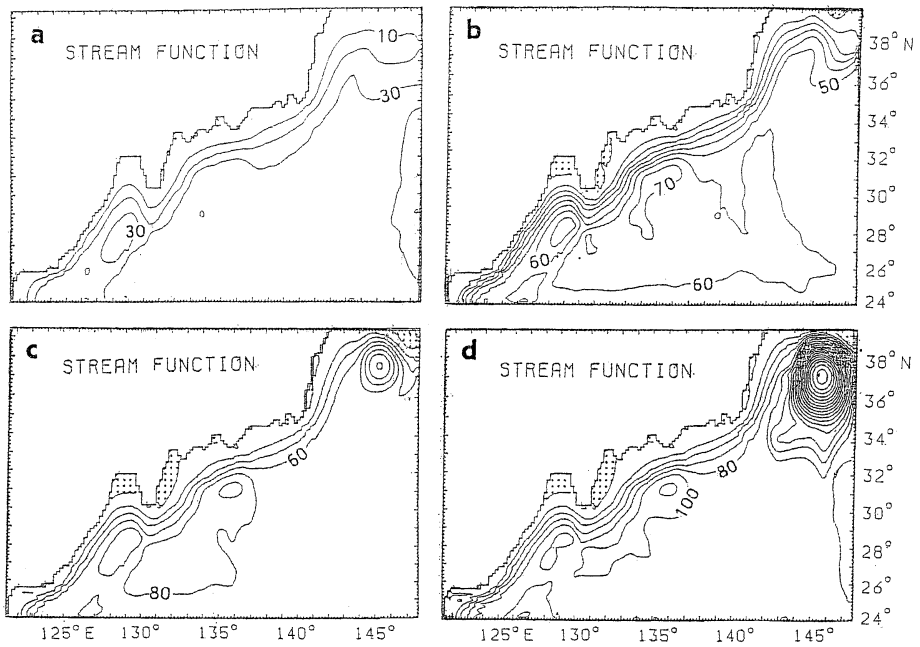

Fig. 8. Volume transport function of (a) T30, (b) T55, (c) T70 and (d) T80 in a stationary state. The contour intervals in T30 and T55 are 10 Sv and those in T70 and T80 are 20 Sv. Areas with negative volume transport function are stippled.

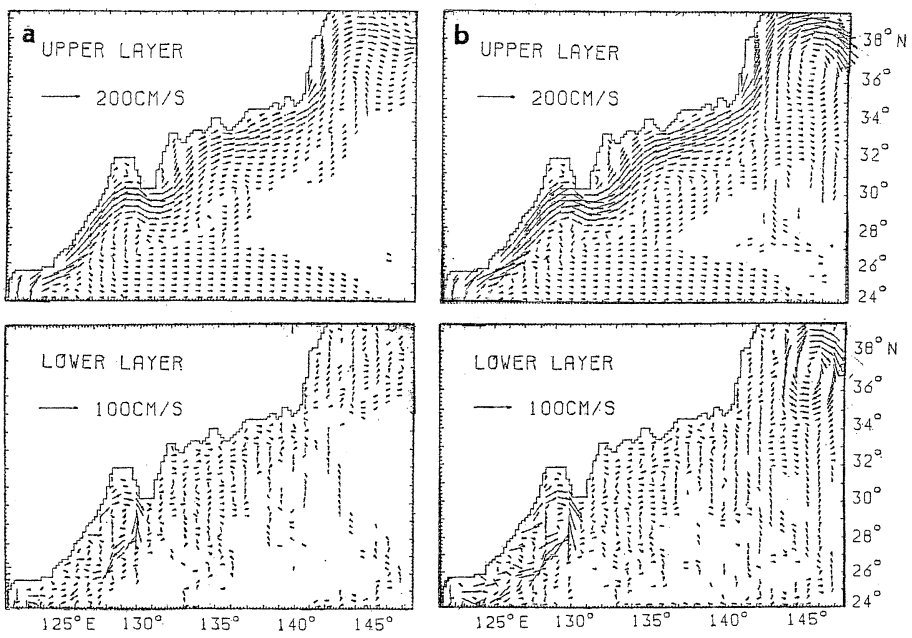

Fig. 9. Same as in Fig. 7 but for (a) T55 and (b) T80.

velocity distribution of the Kuroshio south of Kyushu, as a succeeding study of the numerical experiment of ZHANG and SEKINE (1995a,b). The main results of the present study are summarized as follows:

(1) It is resulted from the numerical experiments that the Tokara Strait is essentially considered as a separation region of the Kuroshio from the western boundary in the East China Sea. An strong anticyclonic eddy is formed in this region in a flat bottom model and the southwestward flow is formed in the lower layer at the southwestern part of the anticyclonic eddy during its spin-down periods.

(2) In the realistic bottom model, the southwestward flow along the continental slope off Nansei Islands is commonly generated by the topographic guiding effect along isopleth of depth. This southwestward flow is an opposite direction to the Ryukyu Current and the Ryukyu Current is blocked by the southwestward flow. Although the Ryukyu Current is essentially formed as a barotropic flow, the vertical shear is observed. It is suggested that the vertical shear of the Ryukyu Current is caused by the blocking of the southwestward flow.

(3) In case of the large meander path, the northward shift of the current path at the western region of the Tokara Strait is clear in the upper layer in comparison with those in the non-large meander path. This agrees with the results of the previous observations and the numerical studies so far proposed. It is suggested that the large meander path is essentially considered as a Rossby Lee wave formed by the coastal topography of Kyushu.

(4) Although the non-large meander path is formed in F80 in ZHANG and SEKINE (1995a), the large meander path is formed in F80 of the present study. As the inflow of ZHANG and SEKINE (1995a) was made at the western region of the Tokara Strait, the eastward advection of the large meander path is enhanced. The range of non-large meander path in exceedingly large current velocity of the Kuroshio is suggested.

On the observed velocity distribution of the Ryukyu Current, it is inferred that the observed confinement of the Ryukyu Current to the shallower margin of the continental slope off Nansei Islands (YUAN *et al.*, 1994; 1998; ZHU *et al.*, 2003) may be generated by the blocking by the southwestward flow denoted in (2). Even if the topographic effect of the continental

slope is weak, the southwestward flow is formed by the spin-down of the anticyclonic eddy mentioned in (1), the residual flow may be exists only in the margin of the continental slope. It is also inferred that because the southwestward flow is formed by the topographic guiding effect of the continental slope off Nansei Islands, the stronger southwestward flow is mainly confined to the lower layer. If the southwestward flow is formed during the spin-down of the anticyclonic eddy, the surface trapped southwestward velocity still exists in the upper layer (Fig. 7a), there is a possibility that the minimum of the southwestward flow exists in the intermediate layer. Therefore, the northeastward Ryukyu Current has a has a maximum velocity at the intermediate layer and the smallest blocking effect is expected in the intermediate layer. This agrees with the observed velocity maximum of the Ryukyu Current at a depth of 600 m (YUAN *et al.*, 1998). However, more detailed discussion is needed to explain the observed velocity distribution of the Ryukyu Current, which will be carried out in the next step of this study.

It is pointed out from (4) that the path pattern of the Kuroshio depends on not only the volume transport but also the velocity distribution at the Tokara Strait. YAMASHIRO and KAWABE (2002) suggested the clear difference in the shape of the Kuroshio axis south of Kyushu between the large meander path periods and the non-large meander path. They also pointed out that a realistic flow through the Tokara Strait should be given in the numerical model, while the inflow should not be given at the Tokara Strait as a boundary condition in almost numerical model so far proposed. The different results between F80 of the present study and that of ZHANG and SEKINE (1995a), which is mentioned in (4), correspond to this event. Therefore, more realistic modeling south of Kyushu including the Ryukyu Current is needed in the next stage of this study.

Acknowledgments:

The numerical calculations were carried out on a VP-2600 in the Computer Center of Nagoya University and on a FACOM M-760 of Mie University Information Process Center. The authors thank Mr. N. Shinoda of Faculty of Bioresources of Mie University, now at Kikusui Co., Ltd. for his help in numerical calculation.

References

AKITOMO, K., T. AWAJI and N. IMASATO (1991): Kuroshio path variation south of Japan. 1 Barotropic inflow-outflow model. J. Geophys. Res., **96**, 2549–2560.

AKITOMO, K., S. MASUDA and T. AWAJI (1997): Kuroshio path variation south of Japan: Stability of the path in a multiple equilibrium regime. J. Oceanogr., **53**, 129–142.

IKEDA, M. (1983): Linear instability of a current along a bottom topography using a three layer model. J. Phys. Oceanogr., **13**, 208–223.

IMAWAKI, S. H. UCHIDA, H. ICHIKAWA, M. FUKASAWA, S. UMATANI and ASUKA Group (2001): Satellite altimeter monitoring the Kuroshio transport south of Japan. Geophys. Res. Let., **28**, 17–20.

ISHII, H., Y. SEKINE and Y. TOBA (1983): Hydrographic structure of the Kuroshio large-cold water mass region down to the deeper layers of the ocean. J. Oceanogr. Soc. Japan, **39**, 240–250.

ISOBE, A. and S. IMAWAKI (2002): Annual variation of the Kuroshio transport in a two-layer numerical model with a ridge. J. Phys. Oceanogr., **32**, 994–1009.

KAGIMOTO, T. and T. YAMAGATA (1997): Seasonal transport variation of the Kuroshio: An OGCM simulation. J. Phys. Oceanogr., **27**, 403–418.

KAWABE, M. (1995): Variation of current path, velocity and volume transport of the Kuroshio in relation with large meander. J. Phys. Oceanogr., **25**, 3103–3117.

NITANI, H.(1975): Variation of the Kuroshio south of Japan. J. Oceanogr. Soc. Japan, **31**, 154–173.

OKA., E. and M. KAWABE (2003): Dynamic structure of the Kuroshio south of Kyushu in relation to the Kuroshio path variation. J. Oceanogr., **59**, 595–608.

SEKINE, Y. (1990): A numerical experiment on the path dynamics of the Kuroshio with reference to the formation of the large meander path south of Japan. Deep-Sea Res., **37**, 359–380.

SEKINE, Y. (1992): On the signs of formation of the Kuroshio large meander south of Japan. Bull. Japan. Soc. Fish. Oceanogr., **56**, 13–22 (in Japanese with with English abstract).

SEKINE, Y. and Y. TOBA (1981a): Velocity variation of the Kuroshio during formation of the small meander south of Kyushu. J. Oceanogr. Soc. Japan, **37**, 87–93.

SEKINE, Y. and Y. TOBA (1981b) A numerical study on the generation of the small meander path of the Kuroshio off southern Kyushu. Journal of Oceanogr. Soc. Japan, **37**, 234–242.

SEKINE, Y. and K. KUTSUWADA (1994): Seasonal variation in volume transport of the Kuroshio south of Japan. J. Phys. Oceanogr., **24**, 261–272.

SOLOMON, H. (1978): Occurrence of small "trigger" meanders in the Kuroshio off southeastern Kyushu. J. Oceanogr. Soc. Japan., **34**, 81–84.

TAFT, B. (1972): Characteristics of the flow of the Kuroshio south of Japan. 165–216, In *Kuroshio, Its Physical Aspects*, ed. by H. Stommel and K. Yoshida, Univ. Tokyo Press.

YAMASHIRO, T. and M. KAWABE (1996): Monitoring of position of the Kuroshio axis south of Kyushu using sea level data. J. Oceanogr., **52**, 675–687.

YAMASHIRO, T. and M. KAWABE (2002): Variation of the Kuroshio axis south of Kyushu in relation to the large meander of the Kuroshio. J. Oceanogr., **58**, 487–503.

YUAN, Y., K. TAKANO, Z. PAN, J. Su, K. KAWATATE, S. IMAWAKI, H. YU, H. CHEN, H. ICHIKAWA and S. UMATANI (1994): The Kuroshio in the East China Sea and the current east of Ryukyu Islands during autumn 1991. La mer, **32**, 235–244.

YUAN, Y., A. KANEKO, J. Su, X.-H ZHU , Y. LIU, N. GOHDA, H. CHEN (1998): The Kuroshio east of Taiwan and in the east China Sea and the current east of Ryukyu Islands during early summer of 1996. J. Oceanogr., **54**, 217–226.

ZHANG, M. and Y. SEKINE (1995a): A numerical experiment on the path dynamics of the Kuroshio south of Japan. Part 1 Coastal topographic effect. La mer, **33**, 63–75.

ZHANG, M. and Y. SEKINE (1995b): A numerical experiment on the path dynamics of the Kuroshio south of Japan. Part 2 Bottom topographic effect. La mer, **33**, 77–87.

ZHU, X.-H., I.-S. HAN, J.-H. PARK, H. ICHIKAWA, K. MURAKAMI, A. KANEKO and A. OSTROVSKII(2003): The northwestward current southeast of Okinawa Island observed during November–2000 to August–2001. Goephys. Res. Lett., **30(2)**, 43–1 –43–4.

Received November 11, 2003
Accepted December 1, 2004